

- Schubert, D., 1972, Geomorphology and glacier retreat in the Pico Bolivar area Sierra Nevada de Merida, Venezuela, *Zeitschr. Gletscherkunde Glazialgeol.* 8:189-202.
- Whittow, J. B., Shepherd, A., Goldthorpe, J.E. & Temple, P.H., 1963, Observations on the glaciers of the Ruwenzori, *J. Glaciology* 4(35): 581-616.
- Wollaston, A.F.R., 1914a, An expedition to Dutch New Guinea, *Geogr. J.* 43(3):248-273.
- Wollaston, A.F.R., 1914b, Mountaineering in Dutch New Guinea, *Alpine J.* 28(205):296-304.
- Wood, W.A., 1970, Recent glacier fluctuations in the Sierra Nevada de Santa Marta, *Geogr. Rev.* 60:374-392.
- Zeller, A.N., 1968, Preliminary investigations on the effects of deglaciation upon the thermoluminescence of rock. In: D.J. McDougall (ed), *Thermoluminescence of geological materials.* London, Academic Press.

IAN ALLISON
Antarctic Division, Australian Government Dept. of Science

GLACIER REGIMES AND DYNAMICS

4.1 THE MEREN AND CARSTENSZ GLACIERS

The Meren Glacier and the Carstensz Glacier, the major valley glaciers, account for about 40 per cent of the total present day ice covered area. Both glaciers have retreated considerably from their recent maximum extent (Chapter 3) but are still the most dynamic ice masses in the region. The detailed glaciological observations undertaken by the Carstensz Glaciers Expeditions were confined to these two glaciers.

The surface topography of the Meren Glacier and the Carstensz Glacier is shown in Fig. 4.2. The ice boundary of the ablation zone of both glaciers was determined by tacheometric survey from a primary network of control stations on rock (see Chapter 2). The northern ice boundary of the Northwall Firn was determined with reference to photogrammetry from the 1942 trimetrogon air photographs and from ground photography of the Carstensz Glaciers Expeditions. Eastern and southern ice boundaries have been estimated from ground and aerial oblique photographs of the CGE.

Surface elevation contours have been drawn from the tacheometric data and from the spot elevations of a network of canes on both glaciers (Fig. 4.1). The cane elevations were found by triangulation from the control stations.

The average surface slope of the Meren Glacier, along a central flow line, is 25 per cent and that of the Carstensz Glacier is 20 per cent, but the distribution of surface slope is markedly different for the two glaciers. The maximum slope on the central flowline of the Meren glacier occurs where the Northwall Firn flows into the Midden Firn, and the accumulation zone (average surface slope ($\bar{\alpha}$) of 30 per cent) is steeper than the ablation zone ($\bar{\alpha}$ = 22 per cent) where the englacial lakes occur. In contrast, the Carstensz Glacier has a relatively flat accumulation zone ($\bar{\alpha}$ = 15 per cent) and a broken ablation zone that increases in slope towards the snout ($\bar{\alpha}$ = 26 per cent).

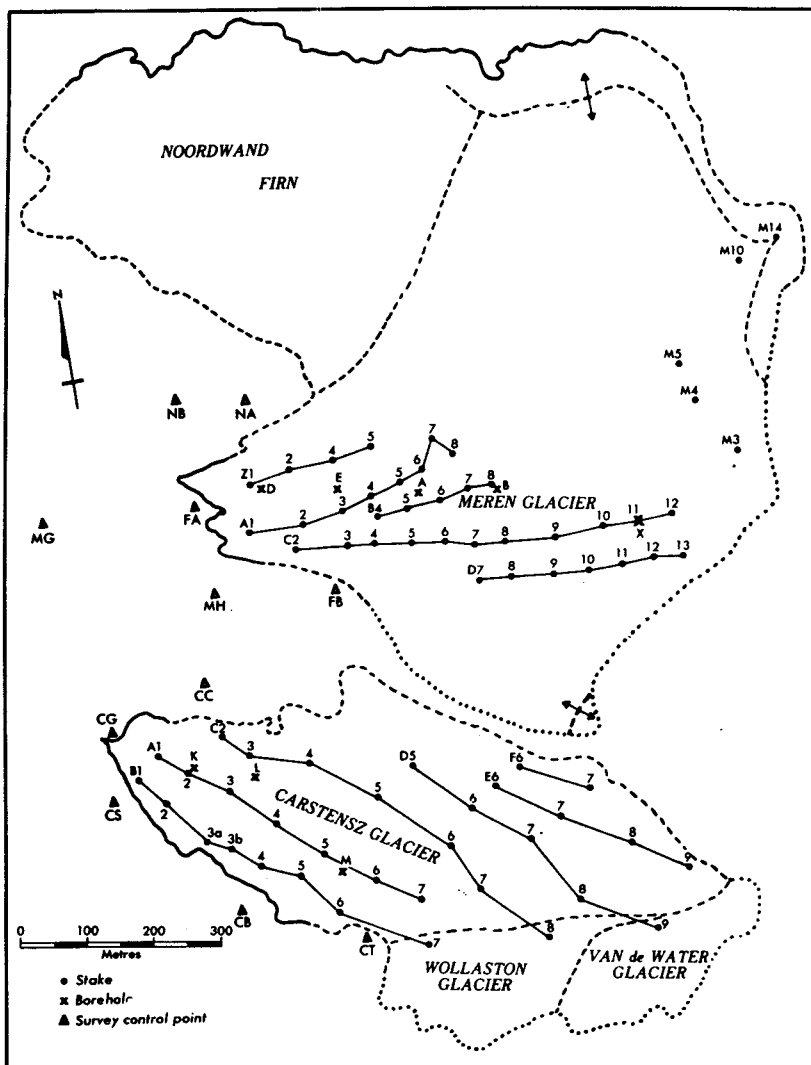


Figure 4.1 Net balance and movement stake networks on the Meren and Carstensz Glaciers

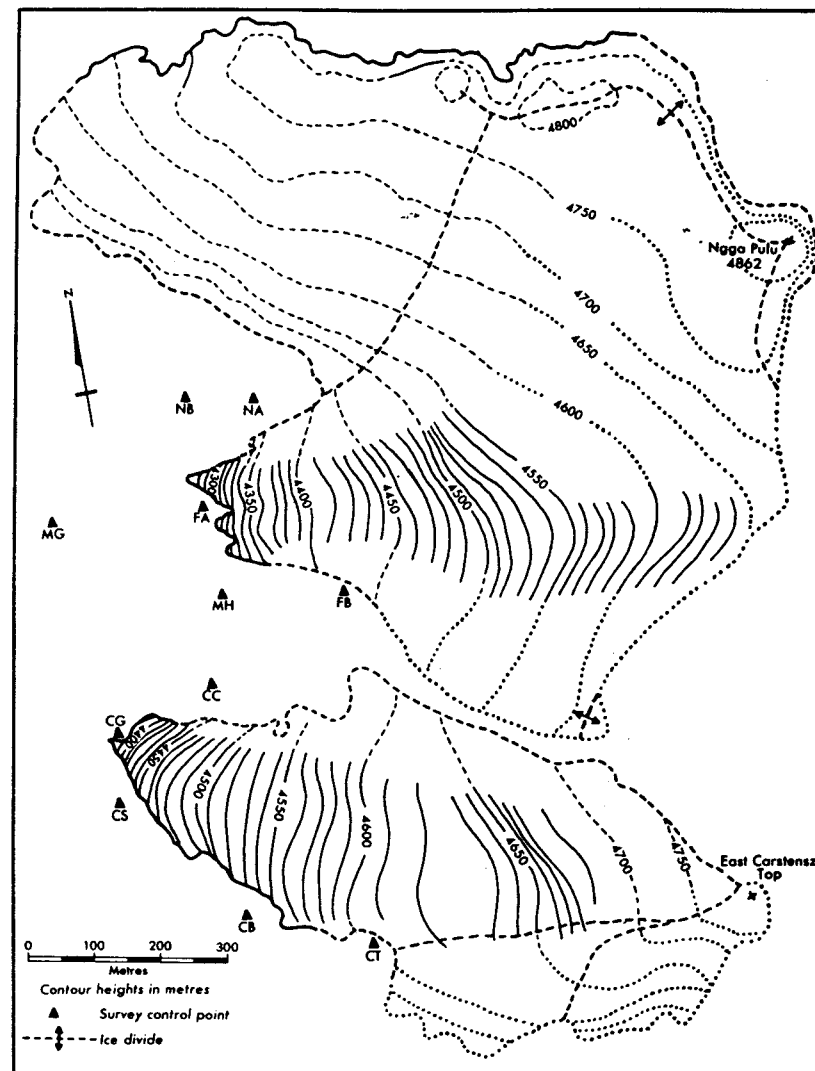


Figure 4.2 Surface topography of the Meren and Carstensz Glaciers
(Reliability: — good, --- fair, poor)

4.2 SURFACE MASS BALANCE

Net balance measurements were made on the network of canes on both the Carstensz and Meren Glaciers. The measurements made at the base camp during the first CGE (Dec. 1971 to March 1972) are presented in Tables 4.1 and 4.2. All values have been converted to water equivalent (w.e.) using an ice density of $0.9 \times 10^3 \text{ kg m}^{-3}$ and a snow density of $0.42 \times 10^3 \text{ kg m}^{-3}$ (the mean of 10 measured snow densities). The plot of net balance against elevation (Fig. 4.3) shows no significant difference in the regime of the two glaciers, both of which face north-west. The equilibrium line for these west-facing slopes during the three-month period was at an elevation of about 4,560 m.

Table 4.1 Net balance data for the Meren Glacier, 24 Dec. 1971 — 5 Mar. 1972 (equilibrium line at approx. 4,560 m)

Stake No.	Elevation (m)	Net balance in mm/day water equivalent (w.e.)								Total No. of days obs.	Average net balance mm/day	Average net balance m/a
		Date of initial measurement and length of observation period (days)										
		24/12	9/1	18/1	26/1	1/2	5/2	12/2	22			
Z1*	4358		-14	-23	-14	-5	-25	-17	56	-17	-6.2	
A1*	4360	-6	-17	-18	-16	-30	-20		50	-14	-5.4	
Z2*	4392		-6	-17	-2	-6	-21	-13	56	-12	-4.2	
A2*	4395	-8	-11	-15	-15	+5	-22		50	-11	-3.9	
C2	4395							-18	13	-18	(-6.7)	
A3*	4415	-14	-10	-13	-17	-7	-6	-15	72	-13	-4.6	
C3	4426							-17	13	-17	(-6.3)	
Z4*	4427		-14	-5	-11	+9	-18	-11	56	-10	-3.6	
A4*	4434	-12	-6	-10	-18	+8	-17	-11	72	-10	-3.7	
B5*	4464	+1	-6	-13	-3	+10	+13	-7	72	-3	-0.9	
A5*	4465		-10	-16	-9	+15	-13	-12	56	-10	-3.7	
Z5*	4469		-5	-8	-6	+2	-5	-12	56	-8	-2.9	
C6*	4484	-15	-4	-10	-7	+3	-15		50	-10	-3.5	
B6	4485			-7	-7	+4	-5		41	-3	-1.0	
A6*	4492	-14	-5	-20	+2	+2	-10		50	-9	-3.3	
D7*	4503	-5	-5	-5	-5	+4	-7		50	-4	-1.6	
B7	4512						-7		7	-7	(-2.6)	
A7	4527	-2	-2						25	-2	-0.7	
B8	4528						-5		7	-5	(-1.8)	
A8	4531	-6	-6	-1	-1	-1	-1		50	-3	-1.3	
C9	4547							-3	29	-3	-1.3	
C10	4578							-1	29	+2	+0.7	
C11	4595							+3	29	+5	+1.8	
D11	4598							+3	29	+5	+1.8	
D12	4613							+3	29	+4	+1.6	
D13	4625							+3	29	+2	+0.8	
Mean of stakes marked *			-9	-13	-9	+1	-13					

Table 4.2 Net balance data for the Carstensz Glacier, 20 Jan. 1972 — 24 Feb. 1972 (equilibrium line at approx. 4,550 m)

Stake	Elevation (m)	No. of days	Mean net balance (water equivalent)	
			mm/day	m/a
A2	4490	30	-2.4	-0.88
A3	4522	30	-2.5	-0.92
C3	4526	35	-4.4	-1.61
B4	4550	31	+0.4	+0.15
A4	4553	35	+1.3	+0.48
C4	4572	35	+2.0	+0.74
B5	4576	31	+1.6	+0.59
A5	4583	35	+2.2	+0.79
B6	4600	31	+3.1	+1.14
C5	4611	35	+4.1	+1.49
A6	4612	30	+3.8	+1.38
B7	4614	31	+2.7	+0.99
C6	4620	30	+2.8	+1.02
A7	4624	30	+2.4	+0.87
C7	4625	27	+3.6	+1.31
D6	4646	27	+4.2	+1.53
C8	4656	27	+4.8	+1.76
E6	4660	28	+5.0	+1.81
D7	4682	27	+4.4	+1.59
D8	4687	27	+4.5	+1.65
F6	4695	29	+4.8	+1.74
E7	4697	27	+5.4	+1.99
D9	4710	27	+4.5	+1.65
E8	4725	27	+6.5	+2.38

The annual net balance (Table 4.3) was measured on the stakes that survived all of 1972. The majority of stakes remeasured were close to the equilibrium line, which was at an elevation of about 4,580 m. The few measurements available for a full year indicate that the annual net balance for 1972 was more negative than the balance obtained by extrapolating the three-monthly values.

Seasonal variations in net balance are difficult to estimate, but are most likely small. No significant stratigraphy was detected in 10 m cores taken from the firnfield of both glaciers. Temperatures at the Ertzberg mine (3,600 m a.s.l.) were recorded with a long-term thermohygrograph between March and September 1972 (Chapter 5) and show less than 0.3°C deviation in the monthly means from the long-term mean of 8.1°C . The annual variation of air temperatures over the glaciers is expected to be even smaller.

Precipitation gauges were installed in the Yellow Valley, at the foot of the Carstensz Glacier, and at the base camp in the Meren Valley during both expeditions, and from March to November 1972 a long-term pluviograph operated in the Yellow Valley. The precipitation data (Chapter 5) show markedly reduced rainfall for the months June to November, but this is thought to be a result of the drought conditions prevailing over New

Table 4.3 Annual net balance data

Meren Glacier			Carstenz Glacier		
Stake	Elevation (m)	Net balance (m/a)(w.e.)	Stake	Elevation (m)	Net balance (m/a)(w.e.)
C9	4547	-0.46	B4	4550	-1.5
C10	4578	+0.29	A4	4553	-1.6
C11	4595	-0.41	C4	4572	+0.01
D11	4598	-0.48	A5	4583	+0.20
D12	4613	+0.53	B6	4600	+0.09
D13	4625	-0.24	C5	4611	-0.08
M3	4690	-0.16	A6	4612	+0.31
M4	4700	+0.01	B7	4614	+0.09
M5	4807	+0.87	C6	4620	+0.22
M10	4710	+0.42	A7	4624	+0.19
M14	4862	+0.93			

Guinea during the latter half of 1972, rather than a seasonal effect. Normally the precipitation regime of the Carstenz area would be expected to be fairly uniform throughout the year, with both the south east trade winds (May to October) and the north east monsoon (December to March) contributing to the accumulation on the glaciers.

Because of the drought, the net balance for 1972 must be considered as atypical. During June, July and early August, New Guinea received a higher than normal frequency of air flow from the south, from over the Australian continent (Bureau of Meteorology 1972). Stations surrounding the Carstenz area show below average precipitation for 1972, with coastal stations to the south, normally influenced by the south east trade winds, receiving up to 50 per cent less rainfall in 1972 (Chapter 5). The discrepancy between the annual and three-month net balance curves in Fig. 4.3 is largely due to the dryness of 1972.

Ablation on the glaciers appears to be predominantly dependent upon radiation. Similar results for other tropical glaciers have been found by Howell (1953) on the Nevado de Huagaruanca (Peru, 10°S) and by Platt (1966) on the Lewis Glacier (Mt. Kenya, 10°S). In the middle reaches of the Lewis Glacier it was found that 90 per cent of the observed melt was due to radiation. On the Meren and the Carstenz Glaciers, melt water run off was significantly greater for cloud free periods than during overcasts. Maximum ablation rates of about 30 mm water equivalent per day were measured during relatively cloudless periods on the snout of the Meren Glacier. Radiation absorption by the glaciers, particularly in the ablation zone, is enhanced by the cryo-vegetation colonies which reduce the surface albedo (Chapter 6).

Because of the high mean humidity (~90 per cent) and low mean wind speed (~2 m/sec) evaporation is small, and ablation is predominantly by melt. No penitentes or sun pits were observed on the glaciers.

The total mass budget for 1972 for the Carstenz and Meren Glaciers is shown in Fig. 4.4. Both glaciers have a negative budget, as would be

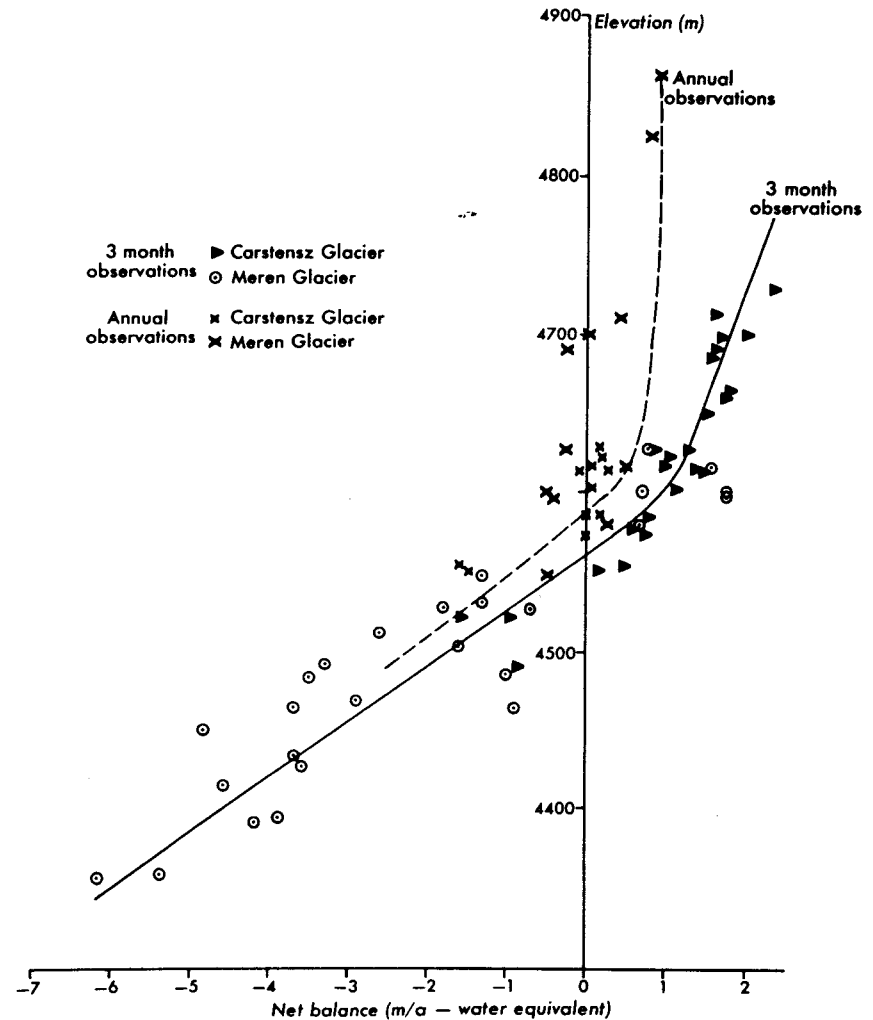


Figure 4.3 Net balance data and profiles for the Meren and Carstenz Glaciers

expected from their continuing retreat. The 1972 mass deficit of the Carstenz Glacier was approximately 57×10^6 kg (an average surface lowering of 0.06 m) and the deficit for the Meren Glacier was approximately 990×10^6 kg (average surface lowering of 0.51 m).

With an equilibrium line elevation of 4,580 m, the accumulation area ratio of the Carstenz Glacier is 66 per cent, and that for the Meren Glacier is 59 per cent.

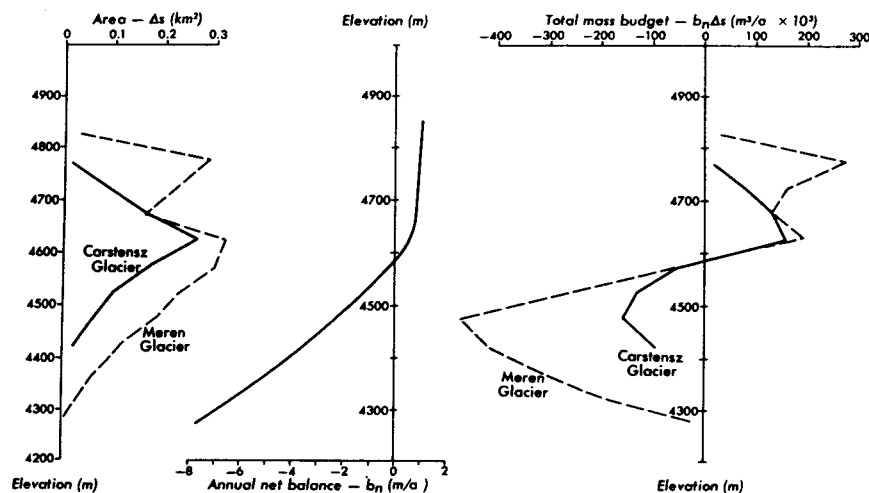


Figure 4.4 Hypsometric curves, net balance profile, and total mass budget (1972) for the Meren and Carstensz Glaciers.

4.3 HYDROLOGICAL MEASUREMENTS ON THE CARSTENZ GLACIER

The hydrological balance for a glacierized basin can be expressed as:

$$R = P - E - \Delta G - \Delta S$$

where R is the total runoff from the basin, P the total precipitation over the basin, E the evaporation and ΔG and ΔS the changes in ground water and snow and ice storages.

A water level recorder and weir were installed on a stream draining melt water from the entire tongue of the Carstensz Glacier and, in conjunction with the pluviograph, this instrument recorded continuously from March till November 1972. Monthly values of total precipitation (P) and runoff are presented in Table 4.4. The constant runoff, despite the decrease in precipitation in the latter half of the year, is probably due to high melt rates consequent upon the low cloudiness accompanying the drought during that period (Bureau of Meteorology 1972).

The hydrology of the Carstensz basin is complicated by subterranean drainage in the limestone bedrock, but no measurements are available of either underground runoff or of changes in the ground water. However, assuming that evaporation is negligible compared to the other processes, then the subterranean processes for the period must equal the $99 \times 10^3 \text{ m}^3$ surplus, plus the decrease in glacier mass between March and November.

Between February 1972 and February 1973 the snout of the Carstensz

Glacier retreated an average of 9 m, involving an ice loss of approximately $10 \times 10^3 \text{ m}^3$. Additional ice loss due to surface lowering of the ablation area was probably of the same order of magnitude. Overall, the underground drainage of meltwater on the Carstensz Glacier is probably about 5 per cent of the total runoff.

4.4 THERMAL REGIME OF THE GLACIERS

Eight 10 m deep boreholes were drilled on the Meren Glacier (at elevations of 4,365 m (Hole D), 4,417 m (E), 4,470 m (A), 4,523 m (B), and 4,595 m (X)) and on the Carstensz Glacier at 4,495 m (Hole K), 4,536 m (L), and 4,595 m (M). The position of the boreholes is shown in Fig. 4.1.

Temperatures were logged down all boreholes using a thermistor probe with an accuracy of $\pm 0.2^\circ \text{C}$. The temperature at 10 m depth in all boreholes lay between -0.1 and -0.2°C and, within the accuracy of the temperature measurements, the ablation zones of both glaciers are temperate. The temperatures in the top 10 m were near isothermal, indicative of the small variation of air temperature throughout the year. On the Meren Glacier, the temperature at 1 m depth in hole X was -0.4°C , whilst the 1 m temperature in hole B was 0.0°C .

The bottom two metres or so of all boreholes on the Meren Glacier filled with melt water very rapidly, often before the coring was completed. The two lower holes (D and E) completely filled with water after a period of overnight rain. On the Carstensz Glacier, where the water drainage is mostly via crevasses and subglacial channels, the holes remained dry.

The highest boreholes on both glaciers were just within the accumulation zones. The transformation of firm to glacier ice occurred at a depth of about $7\frac{1}{2}$ m in borehole X on the Meren Glacier, and at a depth of about 5 m in borehole M on the Carstensz Glacier.

Table 4.4 Runoff and total precipitation for the Carstensz Glacier drainage basin

Month	pptn (m)	Total pptn over area $\text{m}^3 \times 10^3$	Mean monthly stream flow (CuSec)	Total runoff $\text{m}^3 \times 10^3$	Excess pptn over runoff $\text{m}^3 \times 10^3$
March	0.399	463.6	3.15	238.9	+224.7
April	0.304	353.2	3.02	221.7	+131.5
May	0.245	284.7	3.02	229.0	+ 55.7
June	0.155	181.3	3.38	248.1	- 66.8
July	0.242	281.2	3.43	260.1	+ 21.1
August	0.131	152.2	3.45	261.7	-109.5
September	0.170	197.5	3.09	226.8	- 29.3
October	0.125	145.3	3.00	227.5	- 82.2
November	0.151	175.5	3.02	221.7	- 46.2
Total		2234.5		2135.5	+ 99.0

Area of glacier: $894 \times 10^3 \text{ m}^2$ Total area of drainage basin: $1162 \times 10^3 \text{ m}^2$

4.5 ICE DEPTHS AND TOTAL PRESENT DAY ICE VOLUMES

During the first CGE a gravity survey was made on the Carstensz and Meren Glaciers with a Worden gravimeter. Results of this survey have been used to determine ice thicknesses, notwithstanding the difficulties and pitfalls of using gravimetric methods of determining ice thickness in an area of such rugged terrain.

Residual gravity anomalies relative to station MG were calculated after correction for meter drift, elevation differences and terrain effects. The terrain corrections relative to MG, which reach values as high as 44 mgal near the 800 m escarpment at the top of the Carstensz Glacier, were estimated using the graticule method of Hammer (1939) and by assuming that the Bouguer anomaly at all stations on rock was due to terrain effect alone. The absolute terrain correction at MG was about 5.4 mgal.

Ice thicknesses were estimated by assuming the residual anomaly to be due to a semi-infinite slab of ice of density $0.9 \times 10^3 \text{ kg m}^{-3}$, rather than rock of measured density $2.69 \times 10^3 \text{ kg m}^{-3}$. The very large and uncertain terrain corrections, and the fact that no allowance was made for possible cavities and channels in the limestone bedrock, makes the use of a more refined model than that of the semi-infinite slab unwarranted.

The ice depth contours are shown in Fig. 4.5 and the glacier cross-sections in Fig. 4.6 and 4.7. The positions of the transverse cross-section lines are shown on Fig. 4.5, and the longitudinal cross-sections are along the flowlines marked on Fig. 4.8. Both the depth contours and the cross-sections are subject to very large possible errors but, at least for the Carstensz Glacier, the gravimetric ice thicknesses are borne out by numerical modelling of the Carstensz Glacier, using a two-dimensional flowline model (Budd & Jenssen 1975) and reported elsewhere (Allison 1975).

The maximum ice thickness of the Carstensz Glacier is about 75 m and the maximum thickness of the Meren Glacier is about 85 m.

Table 4.5 Total present day ice volumes

Region	Area (km ²)	Mean ice thickness (m)	Volume (km ³ × 10 ⁻³)
Northwall Firm (western portion)	2.5	35	88
Northwall Firm (eastern portion)	1.1	40	44
Meren Glacier	1.95	40	78
Carstensz Glacier	0.89	38	33.8
Wollaston Glacier	0.17	31	5.3
Van de Water Glacier	0.14	15	2.1
Southwall Hanging Glaciers	0.2	15	3
Total	6.9	37	254

From the ice thickness data of Fig. 4.5, and estimated ice thicknesses in other areas, the total ice volume in the Carstensz area has been calculated as 0.25 km³ (Table 4.5).

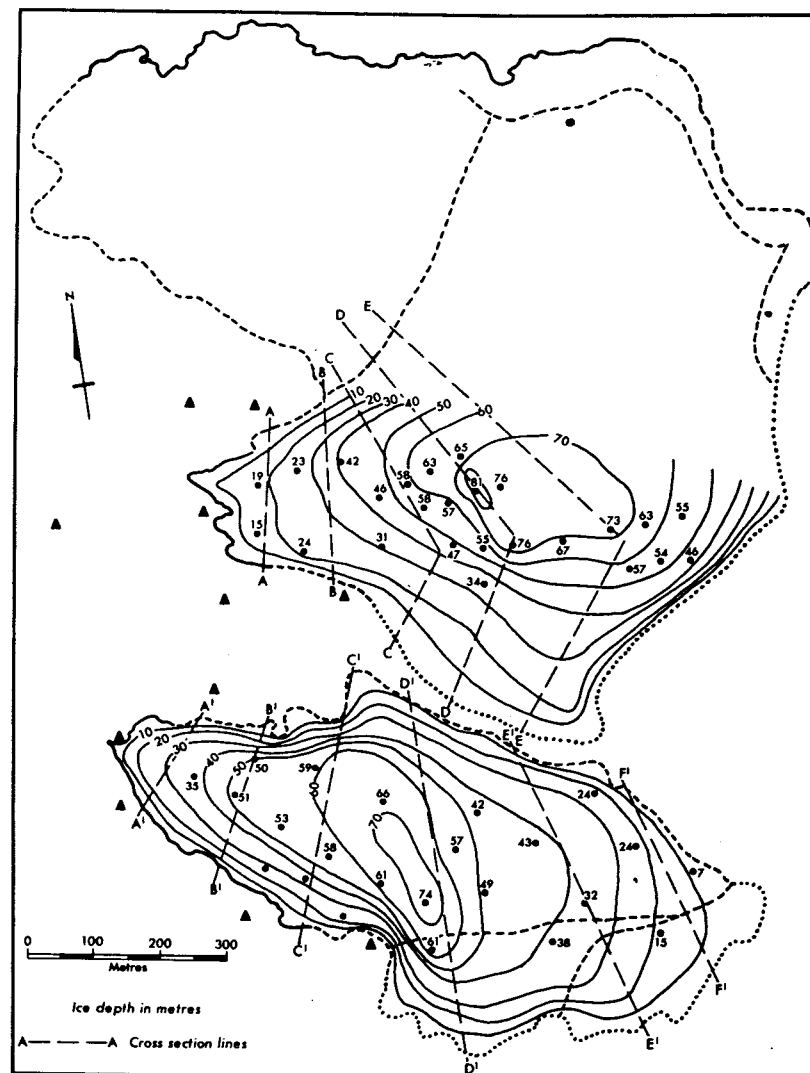


Figure 4.5 Ice depth contours from gravimetry for the Meren and Carstensz Glaciers

4.6 SURFACE ICE VELOCITIES

Surface velocity measurements for the Carstenz and Meren Glaciers were made on the stake networks. The stake positions were fixed with respect to the survey control stations, on rock, using electronic distance measuring equipment (in 1972) and intersection and subtense techniques (in 1973). Stake movements were determined over a period of one to two months during 1972 and over one year for those stakes still extant in 1973. The measured ice velocities are presented in Table 4.6. The accuracy of the velocities measured over one year is about $\pm 2 \text{ m a}^{-1}$ and that of the measurements over two months about $\pm 5 \text{ m a}^{-1}$.

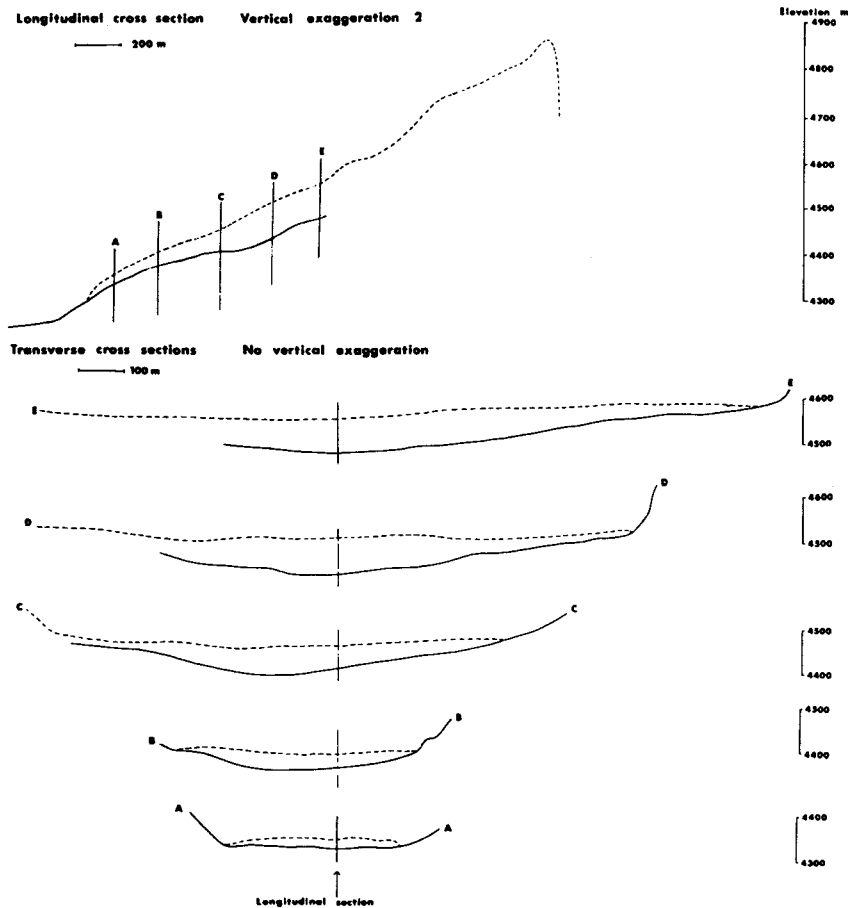


Figure 4.6 Longitudinal and transverse cross-sections of the Meren Glacier

Movement observations were also made on the Meren drill holes over a 17-day period in 1973, and the results are included in Table 4.6. The accuracy of these measurements is discussed in Chapter 2.

All measured surface velocities are plotted on Fig. 4.8. The Meren Glacier, with a steeper surface slope and somewhat greater thickness than the Carstenz Glacier, has an average centre line velocity of about 25 m a^{-1} , and a maximum measured velocity of 34 m a^{-1} . The average centre line velocity on the Carstenz Glacier is 15 m a^{-1} and the maximum measured

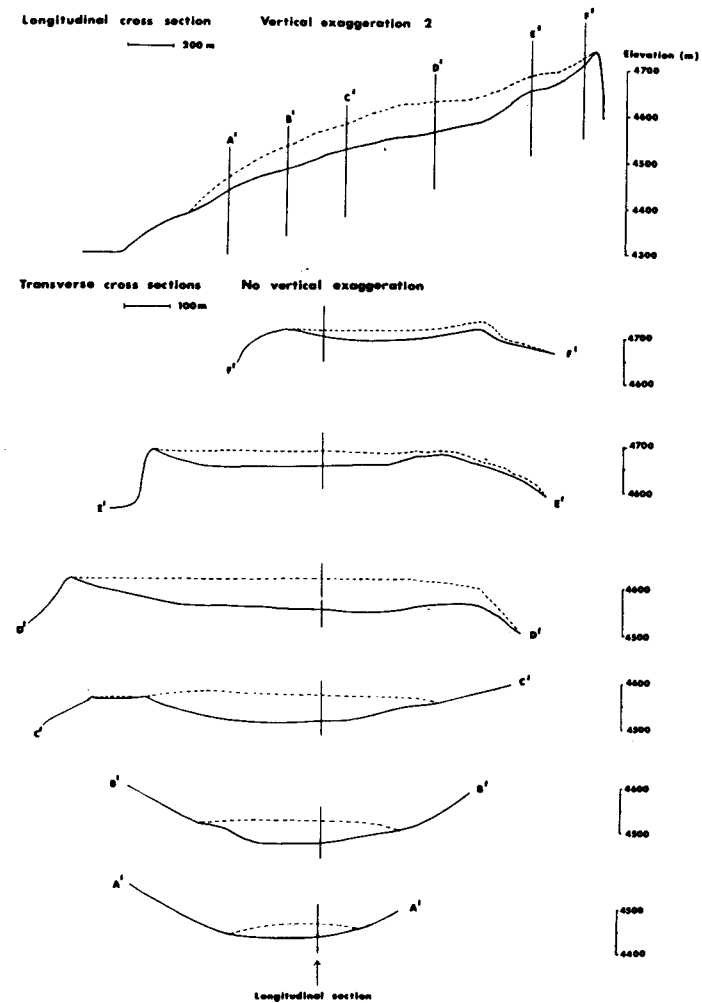


Figure 4.7 Longitudinal and transverse cross-sections of the Carstenz Glacier

velocity was 18 m a^{-1} . Central flowlines, which have been constructed as perpendiculars to the elevation contours, are shown for both glaciers.

Although both glaciers are lubricated by melt water at their bedrock surface, most of the measured velocity is due to internal deformation

Table 4.6 Surface velocities

Stake	Northing	Eastng	Period of measurement	No. of days	Velocity (m/a)	Direction ($^{\circ}$ true)
MEREN GLACIER						
Position 16/2/72						
A3	9851.4	20851.2	24/12/71 - 16/2/72	54	21.6	288
A4	9885.5	20955.2	" "	54	26.3	281
A5	9913.6	21041.2	" "	54	27.3	279
A6	9936.1	2118.4	" "	54	25.2	276
B5	9834.8	21084.6	" "	54	29.3	270
C6	9711.0	21154.1	" "	54	33.9	290
C9	9674.2	21485.4	16/2/72 - 15/2/73	364	10.6	267
C10	9673.9	21634.2	" "	364	4.9	252
C11	9673.9	21727.3	" "	364	2.9	209
Z1	9987.2	20599.6	24/12/71 - 16/2/72	54	17.4	296
Z2	9998.4	20725.9	" "	54	18.7	292
Position 15/2/73						
D	9963.0	20628.2	29/1/73 - 15/2/73	17	16.2	286
E	9907.7	20855.2	" "	17	21.9	271
A	9943.8	21084.0	25/1/73 - 15/2/73	21	17.5	260
B	9810.3	21300.9	29/1/73 - 15/2/73	17	19.3	267
CARSTENSZ GLACIER						
Position 3/3/72						
B1	9154.9	20114.5	22/1/72 - 3/3/72	41	17.4	321
B2	9070.2	20188.4	" "	41	17.8	307
B3a	8948.1	20291.3	" "	41	15.1	298
B4	8847.5	20438.5	3/3/72 - 14/2/73	348	15.5	292
B6	8665.9	20646.4	" "	348	6.0	284
B7	8521.2	20896.9	22/1/72 - 14/2/73	389	15.5	260
A2	9159.0	20262.3	22/1/72 - 3/3/72	41	14.3	315
A3	9082.8	20375.1	" "	41	16.6	306
A4	8963.9	20503.2	23/1/72 - 14/2/73	388	15.3	290
A5	8848.4	20626.5	" "	388	14.7	286
A6	8734.4	20768.5	" "	388	9.6	290
A7	8662.0	20899.8	" "	388	2.2	270
C3	9176.2	20458.3	22/1/72 - 3/3/72	41	14.8	303
C4	9116.7	20637.0	22/1/72 - 14/2/73	389	11.8	272
C5	8983.2	20817.3	" "	389	11.1	276
C6	8814.7	20913.3	" "	389	9.6	280

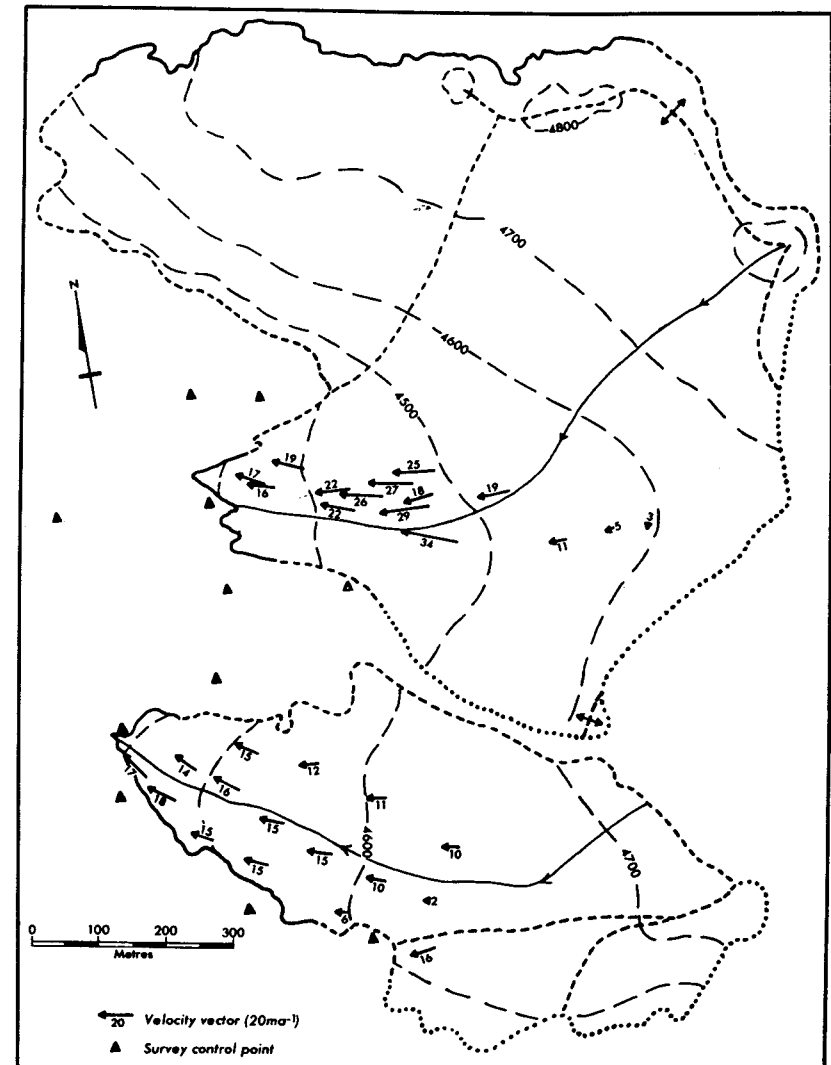


Figure 4.8 Surface velocity vectors and estimated central flowlines on the Meren and Carstensz Glaciers

within the ice rather than basal sliding. Numerical models of the glaciers, with the inclusion of basal sliding parameters, show that the sliding component for both glaciers is less than 0.5 m a^{-1} (Allison 1975).

Computed centreline basal stresses (τ_b) for the Carstenz Glacier are everywhere less than 0.8 bar. Basal stresses have been calculated as:

$$\tau_b = s \rho g z \sin \alpha$$

where

- s is the shape factor (Nye 1965),
- g is the gravitational acceleration,
- ρ is the ice density ($0.9 \times 10^3 \text{ kg m}^{-3}$),
- α is the surface slope,
- z is the ice thickness.

For the Meren glacier, the centre line base stresses vary between 0.5 bar and a maximum, where the Northwall Firn joins with the Midden Firn, of 1.5 bar.

4.7 OXYGEN ISOTOPE MEASUREMENTS

Analyses of the stable isotope of oxygen, ^{18}O , in firn and ice are of considerable glaciological value. The ratio of isotopes, $^{18}\text{O}/^{16}\text{O}$, in fresh precipitation is dependent on the previous meteorological history of the parent water vapour and upon the condensation temperature during precipitation. Thus the ratio in the accumulation on a glacier will vary according to elevation, season, storm path and other factors, and can be used as a natural tracer. On temperate glaciers, the ratios are modified by fractionation and exchange during metamorphism involving meltwater, but still retain some value as tracers (Epstein & Sharp 1959; Sharp et al. 1960).

Oxygen isotope ratio data is usually expressed in terms of a relative deviation, δ , of the heavy isotope content of a sample from that of a standard.

$$\delta = \left(\frac{(\text{H}_2^{18}\text{O}/\text{H}_2^{16}\text{O})_{\text{sample}}}{(\text{H}_2^{18}\text{O}/\text{H}_2^{16}\text{O})_{\text{standard}}} - 1 \right) \times 10^3 \text{ ‰}$$

The reference used is SMOW (Standard Mean Ocean Water, Craig 1961).

Isotope measurements from tropical snowfields are scarce and show large variation. E. Tongiorgi measured δ values in fresh snowfall on the side of Mt. Kilimanjaro (3°S) ranging from -3.7‰ at 4,600 m to -6.8‰ at 5,700 m (Gonfiantini 1970). In contrast, δ values for firn from the Quelccaya ice cap in Peru (5,500 m, 10°S) show a very low mean of -21‰ and an extremely large seasonal range from -11‰ to -33‰ (Thompson & Dansgaard 1975).

The boreholes on the Meren and Carstenz Glaciers provided an opportunity to sample for oxygen isotope measurements to considerable depths along flowlines on the glaciers. Shavings of ice were taken from core lengths of approximately one metre, allowed to melt in small, sealed plas-

tic bottles, and returned to Australia for analysis. One metre of ice from the ablation zone represents several years' accumulation so any seasonal trends in the measured ratios have been averaged out. Because of a shortage of sample bottles, only the top few metres from the Carstenz Glacier were sampled.

The measured isotope ratios are presented in Table 4.7. Repeated measurements were made on each sample and the accuracy of measurement is better than 0.3‰ . The range of δ values measured on the Carstenz Glaciers is -13.6 to -17.2‰ , with a mean δ of all measured ratios of -15.7‰ .

Profiles of δ values down the boreholes are plotted in Fig. 4.9. The

Table 4.7 Oxygen isotope ratios

Sample depth (m)	$\delta^{18}\text{O}$ (‰)	Sample depth (m)	$\delta^{18}\text{O}$ (‰)	Sample depth (m)	$\delta^{18}\text{O}$ (‰)
MEREN GLACIER					
Borehole D (4,365 m)		Borehole E (4,417 m)		Borehole A (4,470 m)	
0.00 - 0.92	-17.1	0.00 - 1.10	-17.1	0.00 - 0.92	-14.6
0.92 - 2.05	-17.2	1.10 - 2.19	-16.9	0.92 - 2.34	-16.1
2.05 - 3.14	-16.5	2.19 - 3.54	-16.8	2.34 - 3.24	-15.6
3.14 - 4.13	-16.4	3.54 - 4.94	-16.7	3.24 - 4.44	-16.0
4.13 - 5.35	-17.1	4.94 - 6.19	-16.7	4.44 - 5.52	-15.0
5.35 - 6.39	-16.6	6.19 - 7.49	-16.3	5.52 - 6.49	-15.2
6.39 - 7.63	-17.2	7.49 - 8.65	-16.3	6.49 - 7.50	-15.9
7.63 - 8.89	-16.8	8.65 - 9.83	-16.6	7.50 - 8.58	-16.3
8.89 - 10.05	-16.4			8.58 - 9.31	-16.0
Borehole B (4,523 m)		Borehole X (4,595 m)		Sample N (4,660 m)	
0.00 - 1.05	-16.0	0.00 - 0.98	-13.7	0.00 - 0.50	-14.5
1.05 - 2.02	-16.3	0.98 - 1.99	-12.7		
2.02 - 3.20	-15.7	1.99 - 3.13	-13.6		
3.20 - 4.36	-16.0	3.13 - 4.19	-14.4		
4.36 - 5.33	-15.8	4.19 - 5.16	-15.2		
5.33 - 6.29	-15.7	5.16 - 6.40	-15.0		
6.29 - 7.42	-16.2	6.40 - 7.73	-15.5		
7.42 - 8.84	-16.4	7.73 - 8.88	-15.3		
8.84 - 10.16	-16.8	8.88 - 9.93	-15.5		
CARSTENZ GLACIER					
Borehole K (4,495 m)		Borehole L (4,536 m)		Borehole M (4,595 m)	
0.00 - 1.50	-15.6	0.00 - 1.40	-16.1	0.00 - 2.00	-14.3
1.50 - 2.95	-15.1	1.40 - 2.90	-15.2	2.00 - 4.00	-13.8
2.95 - 4.50	-15.1	2.90 - 4.37	-14.8		
Sample C1 (4,613 m)		Sample C2 (4,622 m)			
0.00 - 0.50	-14.7	0.00 - 1.20	-14.6		

profiles for the Meren values have been smoothed by taking three-point running means. In the ablation zone, both glaciers show an irregular, but definite increase of δ with altitude of the borehole. Similar variations in δ with altitude are found for other temperate glaciers (e.g. Sharp et al. 1960) and are indicative of a decrease in δ in precipitation with elevation, combined with the typical particle paths in a glacier, with ice lower in the

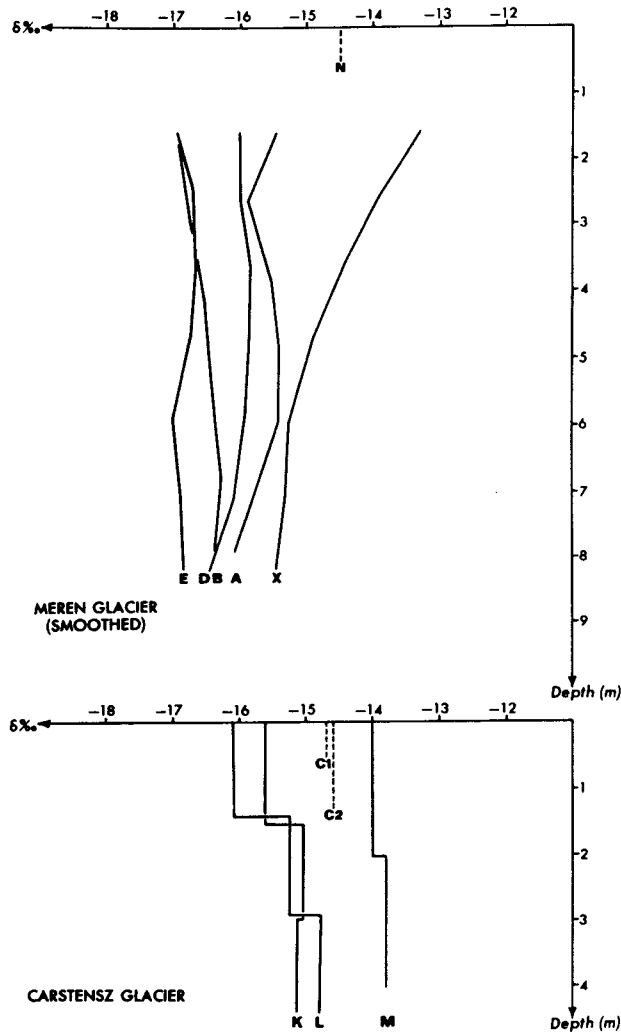


Figure 4.9 Oxygen isotope profiles for glacier ice cores

ablation zone originating from higher in the accumulation zone. The elevation effect in fresh snowfall was not measured but, assuming that the lowest Meren ice (borehole D, $\delta = -16.7\text{‰}$) originated from an elevation of about 4,800 m, and that ice in the lower part of borehole X ($\delta = -15.5\text{‰}$) originated not far above its present elevation (4,600 m), then the elevation effect on isotopic composition in the area is about 0.6‰ per 100 m. Such an estimate makes no allowance for either secular climate change, or decrease in surface elevation, in the time taken for ice at D to flow the full length of the glacier (approx. 100-200 years), both of which would tend to decrease the estimate. The estimated elevation effect is however, of a comparable magnitude to that found in other regions (Dansgaard 1964).

Both glaciers show considerable difference in the isotopic content of firn (boreholes X and M) from that of ice in the ablation zone. The firn samples are greatly enriched in the heavy isotope compared with the ice samples, and the profile for borehole X shows a gradual depletion of the heavy isotope with age, down to the level at which the firn turns to ice (about 7 m).

This result is somewhat surprising in the light of measurements on other temperate snowfields (Sharp et al. 1960; Arnason 1970; Ambach et al. 1972), all of which show enrichment in the heavy isotope during metamorphism, due to the percolation of melt water through the pack. Although the depletion of ^{18}O in the Meren firn cannot be fully explained, a number of possible causes are suggested.

A continuous climatic warming in very recent times would explain the observed firn profile, but is highly unlikely as a cause. The warming rate required to give the observed ^{18}O depletion is of the order of 3.5°C in the period of five years or less (the approximate time for the firn to be transformed into ice).

Dansgaard (1964) shows that, particularly for tropical stations, there is a negative correlation between δ and the amount of precipitation. Hence precipitation in a drought year might be expected to be enriched in ^{18}O relative to a year with more normal precipitation. However precipitation records for stations surrounding the Carstensz area (Chapter 5) do not show abnormally low rainfall for the few years preceding 1972, and consequently the 'amount effect' cannot explain the continuous ^{18}O depletion with depth shown in the firn from borehole X.

The most likely cause of the ^{18}O depletion lies in the origin of different precipitation forms in the area. Much of the snowfall is associated with cyclonic activity, whereas the daily convective clouds bring mainly rain. If the water vapour in the convective air mass were to have a considerably lower δ than that in the cyclonic air, and hence that in the snow, then exchange between the firn and percolating water from convective rain, or between the moist convective air and free water in the snow pack, would deplete the heavy isotope concentration in the firn. The convective air mass might be expected to have a low δ if it is subject to continuous condensation during its uplift, since water vapour preferentially loses the heavy isotope component by condensation, and δ of newly formed precipitation, and of

the remaining vapour, will get more and more negative with further condensation (Dansgaard 1964).

In addition to the core measurements, a few shallow firn samples were analysed. The δ values for these samples are shown in Fig. 4.9 and, in general, they show the expected decrease of δ from that of surface samples near the firn line (boreholes X and M) with increasing elevation in the accumulation zone.

4.8 CONCLUSIONS

The Carstensz area contains one of the few extensive snowfields in the tropical zone, and the Carstensz and Meren Glaciers are unique as thermodynamically temperate, tropical valley glaciers. Despite their continual retreat within the past century, and their present small size, both glaciers must be classified dynamically as active.

With their present mass budget, both glaciers will continue to retreat. The Meren Glacier, in particular, is in danger of losing its form as a valley glacier, and degenerating into an extension of the Northwall Firn, within the next 50 years. The knowledge of the morphology, dynamics and regime of the glaciers, obtained by the CGE, provides a background for continued monitoring of their 'state of health'.

A detailed investigation of the stable isotopes in the Carstensz area, and in particular of the apparent depletion of the heavy isotope during firnification, would be valuable. If, as suggested, the depletion is due to different air masses in the region having greatly different δ values, then stable isotopes will be useful as tracers of the source of precipitation.

4.9 ACKNOWLEDGEMENTS

Support and helpful discussions in formulating the glaciology program, and in analysing the results, were given by W. F. Budd (Antarctic Division) and U. Radok. The oxygen isotope measurements were made by J. Wilson and V. I. Morgan (Antarctic Division) and numerical modelling of the glaciers was undertaken by P. Kruss (Meteorology Department, University of Melbourne). Much of the data for this, and the following chapter, was reduced by Rowan Frew. All members of both expeditions contributed directly to the glacier observations.

4.10 REFERENCES

- Allison, I., 1975, Morphology and dynamics of the tropical glaciers of Irian Jaya, *Zeitschr. Gletscherkunde Glazialgeol.* 10:129-152.
Ambach, W., Eisner, H. & Pessi, K., 1972, Isotopic oxygen composition of firn, old snow and precipitation in alpine regions, *Zeitschr. Gletscherkunde Glazialgeol.* 8:125-135.

- Arnason, B., 1970, Exchange of deuterium between ice and water in glaciological studies in Iceland, *Isotope Hydrology*:59-71. Vienna, IAEA.
Budd, W. F. & Jenssen, D., 1975, Numerical modelling of glacier systems, *Symp. on Interdisciplinary Studies of Snow and Ice in Mountainous Regions*, XV General Assembly of IUGG, Moscow, August 1971. IASH Pub. 104:257-291.
Bureau of Meteorology, 1972, The drought in the Papua New Guinea highlands during the period June to September 1972, Working Paper 161. Bureau Meteorology, Dept. Science, Australia.
Craig, H., 1961, Standard for reporting concentrations of deuterium and oxygen-18 in natural waters, *Science* 133:1833-1834.
Dansgaard, W., 1964, Stable isotopes in precipitation, *Tellus* 16(4):436-468.
Epstein, S. & Sharp, R. P., 1959, Oxygen-isotope variations in the Malaspina and Saskatchewan Glaciers, *J. Geol.* 67:88-102.
Gonfiantini, R., 1970, Discussion, *Isotope Hydrology*:56. Vienna, IAEA.
Hammer, S., 1939, Terrain corrections for gravimeter stations, *Geophysics* 4(3):184-194.
Howell, W. E., 1953, Measurements of ablation, melting and solar absorption on a glacier in Peru, *Trans. Am. Geophys. Un.* 34(6):883-888.
Nye, J. F., 1965, The flow of a glacier in a channel of rectangular, elliptic or parabolic cross-section, *J. Glaciology* 5(41):661-680.
Platt, C. M., 1966, Some observations on the climate of Lewis Glacier, Mount Kenya, during the rainy season, *J. Glaciology* 6(44):267-288.
Sharp, R. P., Epstein, S. & Vidziunas, I., 1960, Oxygen-isotope ratios in the Blue Glacier, Olympic Mountains, Washington, USA, *J. Geophys. Res.* 65(12):4043-4059.
Thompson, L. G. & Dansgaard, W., 1975, Oxygen isotope and microparticle studies of snow samples from Quelccaya Ice Cap, Peru, Antarctic, *J. U.S.* 10(1):24-26.